

Context-Enhanced Memory-Refined Transformer for Online Action Detection

Zhanzhong Pang
National University of Singapore
pang@comp.nus.edu.sg

Fadime Sener
Meta Reality Labs
famesener@meta.com

Angela Yao
National University of Singapore
ayao@comp.nus.edu.sg

Abstract

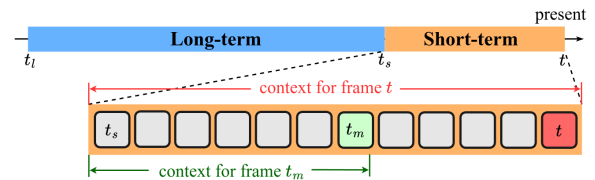
Online Action Detection (OAD) detects actions in streaming videos using past observations. State-of-the-art OAD approaches model past observations and their interactions with an anticipated future. The past is encoded using short- and long-term memories to capture immediate and long-range dependencies, while anticipation compensates for missing future context. We identify a training-inference discrepancy in existing OAD methods that hinders learning effectiveness. The training uses varying lengths of short-term memory, while inference relies on a full-length short-term memory. As a remedy, we propose a Context-enhanced Memory-Refined Transformer (CMeRT). CMeRT introduces a context-enhanced encoder to improve frame representations using additional near-past context. It also features a memory-refined decoder to leverage near-future generation to enhance performance. CMeRT¹ achieves state-of-the-art in online detection and anticipation on THUMOS'14, CrossTask, and EPIC-Kitchens-100.

1. Introduction

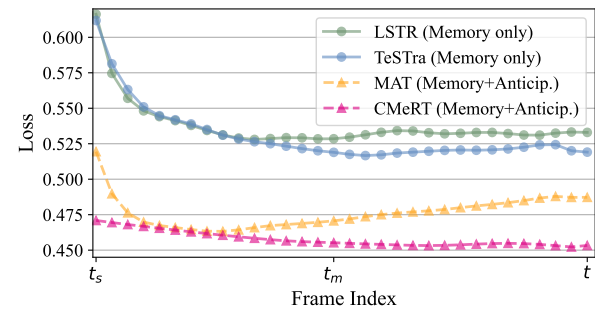
Online Action Detection (OAD) identifies actions in a video stream based on only past observations. This task is crucial for applications like autonomous driving [23], surveillance [34, 41], and AR assistants [4, 12, 25, 38, 39, 56], where immediate and accurate detection is essential.

Effective OAD requires sufficient temporal support from past frames. Recent methods [8, 21, 45, 51, 55] partition past observations into long- and short-term memories, and enrich frames in short-term memory with both immediate and long-range contexts to capture a range of temporal dependencies. A causal mask [44] is typically applied to short-term frames, restricting each frame to access only previous frames so that predictions rely solely on past. This causal masking makes each frame in short-term memory function as if it were the most recent observed frame, allowing all short-term frames to be used as training samples to improve training efficiency. State-of-the-art OAD approaches [8, 21, 45] further leverage action anticipation to generate pseudo-futures, compensating

¹Code: <https://github.com/pangzhan27/CMeRT>.



(a) Imbalanced context exposure in short-term memory, where frames can only access the past: current frame t has full short-term context ($t_s \sim t$), while intermediate frame t_m has only partial ($t_s \sim t_m$).



(b) Frame losses within the short-term memory, showing learning biases toward earlier and intermediate frames.

Figure 1. Existing methods exhibit poorly learned frame representations due to imbalanced context exposure and non-causal leakage.

for the absence of a true future context in OAD. In these works, all frames in the short-term memory are used for training, with each frame having different level of immediate context. However, inference relies exclusively on the *latest frame*, which has access to the full short-term context.

In this paper, we identify a training-inference discrepancy present in state-of-the-art OAD methods and reveal how this discrepancy introduces biases into training, limiting effective modeling of the *latest frame* for inference. As shown in Fig. 1, we observe two sources of bias. (1) The causal mask applied to the short-term memory exposes frames to imbalanced amounts of context relative to frame position. While the latest frame t has full short-term context, the earliest t_s has none due to its position. This imbalance in context degrades learning quality, resulting in less informative representations (large loss) for earlier frames in all SOTA models [45, 51, 55]. These poor representations hinder the classifier’s ability to effectively predict the latest frame. (2) Using anticipation as the pseudo-future to enrich short-term

memory introduces learning biases across short-term frames. Since anticipated context is derived from the full short-term memory, early frames indirectly access their future short-term frames through interaction with anticipation, creating non-causal leakage. This leakage skews training by favoring intermediate frames, which have access to both past and future context. MAT [45] exhibits a valley-shaped loss curve, indicating a learning bias toward intermediate frames, which harms the training and inference of the latest frame.

Based on these key findings, we revisit memory-based OAD methods and focus on mitigating the observed training-inference discrepancy. Building upon the long- and short-term formulation, we introduce the Context-enhanced Memory-Refined Transformer (CMERT). CMERT incorporates a context-enhanced module to supplement the context for earlier frames in short-term memory, improving training and yielding better frame representations. In addition, CMERT includes a memory-refinement module that enhances short-term memory using generated near-future frames. Unlike [45], our anticipated future is derived from long-term memory, preventing non-causal leakage and reducing the learning bias toward intermediate frames.

We also present new protocols for OAD, highlighting several weaknesses in the OAD literature, such as outdated features, limited evaluation metrics, and constrained datasets, which collectively hinder advancements in the field. We evaluate all state-of-the-art OAD methods using stronger visual features [33], implement event-based metrics for better action-level performance assessment, and provide extra comparisons on CrossTasks, a procedural activity dataset where modeling long-term dependencies is essential.

Our contribution are

- revealing a training-inference gap of current OAD approaches, caused by naive memory and anticipation processing.
- proposing a new OAD architecture CMERT with improved memory and anticipation formulations to mitigate the training-inference discrepancy.
- presenting a new OAD benchmark, along with new protocols to update the data, features, and metrics of OAD.
- achieving SOTA detection and anticipation performance on three challenging datasets, under both the standard and our newly proposed protocols.

2. Related Work

Online Action Detection and Anticipation. Early works focus on effectively leveraging past information to model long-range temporal interactions. RNN-based methods [2, 10, 13, 17, 29, 50] model sequences recurrently but struggle to capture long-range dependencies. Techniques like two-stream networks [10], IDN [13], and GatedHub [8] improve temporal modeling, while approaches like [17, 18, 40] decompose the tasks into action recognition and action start

point detection. Some works integrate online detection and anticipation, leveraging a predicted future to improve action detection. These methods employ RNN cells [24, 50] or Transformers [45, 49] for future anticipation.

Transformers for Online Action Detection. Transformers have shown great success in vision [1, 32, 48] and video tasks [3, 7, 31, 54]. Recently, LSTR [51] and TeSTra [55] explore long- and short-term memories using transformers for OAD. These approaches partition the entire history into long- and short-term memories, and use transformers for long-term compression [28, 51], short-long term interactions, future action anticipation [21, 45]. However, these memory-based methods fail to consistently model frames in short-term memory and introduce non-causal leakage when using anticipation results to enhance detection.

In this paper, we systematically analyze short-term memory modeling and joint detection-anticipation, proposing an optimal transformer-based solution. We also advance OAD research using SOTA features, more representative metrics, and a new benchmark on a procedural activity dataset, opening avenues for OAD in new task settings [6, 30] and applications [26, 35, 36].

3. Diagnosing Context Modeling for OAD

3.1. Preliminaries

Online Action Detection identifies the ongoing action at time t in a video stream, relying solely on observations up to and including t . Formally, given a video stream up to t as $V = \{v_0, v_1, \dots, v_t\}$, the objective is to predict the action, $y_t \in \{0, 1, 2, \dots, C\}$, where 0 represents a background class, and y_t is the action in frame t .

Recent memory-based methods LSTR [51] and TeSTra [55] employ transformers. They operate on pre-extracted frame-wise features², $f_t \in \mathbf{R}^D$, and partition the history into short, $M_S = \{f_i\}_{i=t_s}^t$, and long-term memories, $M_L = \{f_i\}_{i=t_l}^{t_s-1}$, to capture both immediate and long-range dependencies. The memory bounds are defined by $t_s = t - T_s + 1$, $t_l = t - T_l - T_s + 1$ where T_s and T_l denote the lengths of short- and long-term, respectively (see Fig. 2). The long-term memory is compressed into a latent representation using transformers with learnable queries [21, 28, 51].

To enhance training efficiency, all frames in the short-term memory are used as training samples, leveraging the same precomputed short- and long-term memories (computed only once). To ensure causality, a mask is applied to the short-term memory, restricting each frame to access only previous frames and make predictions as if it were the most recent observed frame. The short-term frames are enriched by interacting with both their immediate past frames from the short-term memory and the compressed long-term memory.

²Feature extractors typically operate on short segments of consecutive frames. We abuse the term ‘‘frame’’ as segment-wise features for simplicity.

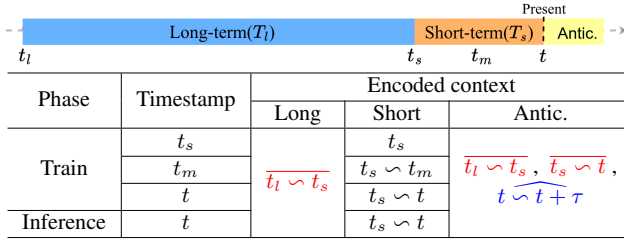


Figure 2. Context analysis for short-term frames. $\overline{~}$ for indirectly encoded, \ast for generated, and the rest for direct context.

In the memory-based setting, training involves sampling a “current” timestamp t , with long and short-term memories constructed by padding or cropping past observations up to t . t is sampled either by (1) a sliding window with a random start time and stride equal to the short-term length, T_s , and (2) event-based sampling, where t is randomly chosen within the duration of a non-background action. In both cases, all frames in a short-term memory serve as training samples to enhance efficiency. During inference, a sliding window with stride 1 and fixed start time at 0 simulates an online streaming setup, predicting one new frame at a time.

Online Action Anticipation predicts the future action occurring after an interval, τ , i.e. $a_{t+\tau} \in \{0, 1, 2, \dots, C\}$, where $a_{t+\tau}$ is the anticipated action in frame $t + \tau$, based on visual evidence up to t . Online action detection is a special case with $\tau = 0$. Thus, recent approaches [21, 45] integrate detection and anticipation within a unified network and utilize anticipation outputs as pseudo-future to improve detection.

3.2. Long- and Short-term Memories

Since all frames in a short-term memory serve as training samples, we first analyze the context accessible to each frame. We use t_s , t_m and t , representing the start, middle, and end of the short-term memory. For **short-term context**, frames t_s , t_m and t access varying amounts of short-term history due to the causal masking (Fig. 2). Frame t has access to the entire short-term memory from t_s to t , while t_s accesses only itself due to its start position, and t_m accesses frames from t_s to t_m . For **long-term context**, the long-term memory M_L is compressed into a latent representation \widehat{M}_L . As a result, all three frames t_s , t_m and t can only access the long-term M_L indirectly through \widehat{M}_L . This compression leads to loss of finer details, preventing frame t_s from recovering its immediate past, despite interacting with \widehat{M}_L .

We observe that short-term frames exposed to varying contexts exhibit different learning behaviors. As shown in Fig. 1 (b), loss curves of short-term memory for existing memory-based models [45, 51, 55] reveal that earlier frames, like t_s and those immediately following, incur higher loss due to insufficient immediate context, resulting in less informative representations. Despite this, these models treat all short-term frames equally during training, with poorly represented frames being low-quality samples. These samples

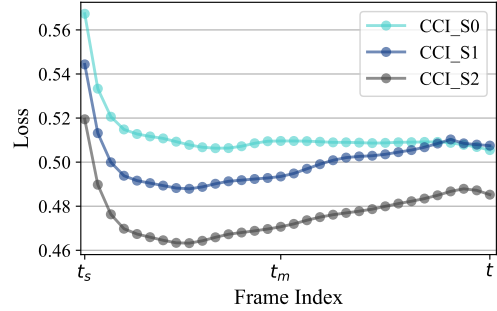


Figure 3. Frame losses within the short-term memory in MAT [45] at different rounds of accessing anticipated future.

ultimately impair the classifier’s ability to effectively predict the latest frame, which is the focus during inference.

Another observation is that for methods that do not use anticipation, such as LSTR [51] and Testra [55], their loss curves in Fig. 1 (b), show that extra context beyond the immediate history offers limited benefits. For example, frames t_m and t both have access to an immediate past of at least $T_s/2$ frames. Yet the extra context available to frame t preceding t_m provides no benefit, suggesting that excessive immediate context may not be necessary.

3.3. Pseudo-Future Context

Building on LSTR [51], MAT [45] unifies anticipation and detection by using anticipation to generate a pseudo-future for frames $t + 1 \sim t + \tau$, to improve detection. MAT introduces Conditional Circular Interaction(CCI) to enable iterative interaction between short-term and anticipation. However, we uncover that its CCI allows short-term frames to indirectly access subsequent frames, compromising the causal nature of OAD and also leading to less informative representations for the later frames.

As shown in Fig. 2, anticipation output is generated based on compressed long and short-term memory via cross-attention. This indirectly incorporates information from the entire short-term memory from t_s to t . When updating the short-term memory with anticipation, earlier frames, such as t_m , indirectly access subsequent frames (t_m to t) through queries to the anticipated future, resulting in non-causal leakage. As such, MAT exhibits higher losses for current frames than intermediate ones, suggesting a learning bias towards intermediate frames, as shown in Fig. 1. This bias is further confirmed in Fig. 3, where learning initially focuses on the current frame without interacting with the anticipated future (CCI_S0), then shifts towards intermediate frames after several rounds of accessing anticipation (CCI_S2).

4. CMERT

We propose Context-enhanced Memory-Refined Transformer (CMERT), a unified framework for detection and anticipation(see Fig. 4) that addresses the imbalanced contexts and learning biases outlined in Sec. 3. Building upon

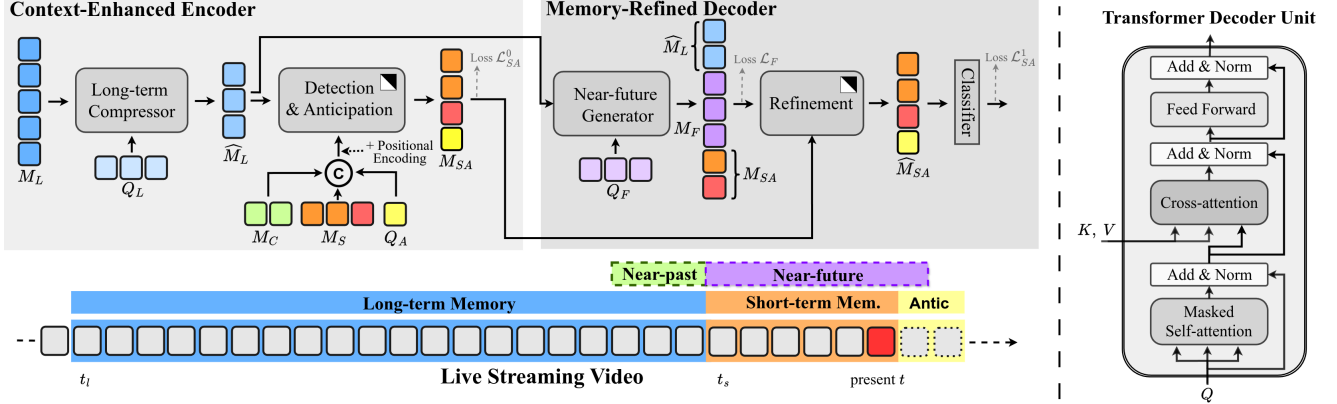


Figure 4. Framework of Context-Enhanced Memory-Refined Transformer. The model is in an encoder-decoder formulation, operating on five context partitions: long-term, short-term, anticipation, near-past, and near-future. The Context-Enhanced Encoder compresses the long-term memory M_L and encodes the short-term memory with anticipation as M_{SA} using the compressed long-term \widehat{M}_L and near-past context M_C . The Memory-Refined Decoder generates the near-future context M_F from \widehat{M}_L and refines M_{SA} using M_F . A weight-shared classifier is adopted to classify both short-term M_{SA} and \widehat{M}_{SA} and near-future M_F . All modules are build upon Transformer Decoder Unit.

[51, 55], we maintain three non-overlapping context partitions: long-term memory, short-term memory, and anticipated context. In addition, we introduce near-past and near-future contexts to mitigate the training-inference discrepancy caused by biases in frame representation learning. CMERT comprises a Context-Enhanced Encoder (Sec. 4.2) and a Memory-Refined Decoder (Sec. 4.3). The encoder leverages near-past context to learn consistent short-term representations, while the decoder queries generated near-future context with these learned short-term representations for decoding. The transformer decoder unit [44] serves as the basic building block (Sec. 4.1) of CMERT.

4.1. Transformer Decoder Unit

Our model uses a Transformer Decoder Unit (TDU) as the core building block, as illustrated in Fig. 4. The TDU takes in queries Q , keys K , values V , and a mask G as input and outputs updated queries \widehat{Q} based on keys and values.

$$\widehat{Q} = \text{TDU}(Q, K, V, G) \quad (1)$$

The TDU consists of a self-attention module for query interactions, a cross-attention module for query-key-value interactions, and a feed-forward network (FFN) for processing the attended information. Each module is followed by a skip connection and LayerNorm [44].

$$\begin{aligned} Q' &= \text{Self-Attention}(Q, G) + Q \\ Q'' &= \text{Cross-Attention}(Q', K, V) + Q' \\ \widehat{Q} &= \text{FFN}(Q'') + Q'' \end{aligned} \quad (2)$$

4.2. Context-Enhanced Encoder

As discussed in Sec. 3.2, earlier short-term frames lack immediate context, resulting in poor representations. The Context-Enhanced Encoder addresses this by incorporating near-past context, improving early frames' representations

and overall learning effectiveness. Our encoder comprises a long-term compressor and a detection & anticipation module. It compresses long-term memory to improve efficiency, then encodes short-term memory based on the compressed long-term and the near-past context. The encoded short-term memory serves as the queries to the Memory-Refined Decoder, rather than being the final output.

Long-term Compression. Given video features up to time t as $F = \{f_i\}_{i=0}^t$, long-term memory stores features $M_L = \{f_i\}_{i=t_i}^{t_s-1}$. For computational efficiency, M_L is first uniformly sub-sampled at a coarse temporal scale. Following prior work [51], a two-stage compression module is applied to M_L to generate an abstract representation \widehat{M}_L . Each stage uses a TDU with learnable queries Q_L for compression. Positional encoding is omitted since the compression process removes temporal information.

$$\begin{aligned} M'_L &= \text{TDU}(Q_L^0, M_L, M_L, \text{None}) \\ \widehat{M}_L &= \text{TDU}(Q_L^1, M'_L, M'_L, \text{None}) \end{aligned} \quad (3)$$

where "None" indicates that no mask is applied.

Detection & Anticipation. Our Detection & Anticipation module employs a TDU with masked self-attention [45, 51]. Here, a causal mask, G , should be applied to the short-term memory to ensure each frame only accesses preceding frames. This causal masking, however, causes an imbalance in immediate context across frames (see Fig. 1 and Fig. 2). To address this, we extract near-past memory, $M_C = \{f_i\}_{i=t_s-T_c}^{t_s-1}$ and append it to the short-term memory to provide extra immediate context for earlier frames at time t_s . Here, T_c represents the near-past context length and $T_c \ll T_l$. While the near-past context, M_C , and the long-term memory, M_L , overlap, the compression applied to the long-term memory M_L loses fine-grained details, which are retained in the extended short-term memory M_C . For anticipation, learnable queries Q_A of length T_a are used.

Finally, M_C , M_S and Q_A are concatenated and passed to the TDU, with sinusoidal positional encoding [44] added to preserve their temporal structure.

Overall, short-term frames are updated through masked self-attention with their immediate past (M_c and M_s), as well as cross-attention with the long-range past (\widehat{M}_L). After contributing additional context, the updated near-past memory is discarded from the TDU output, yielding M_{SA} as the anticipated, updated short-term memory.

$$M_{SA} = \text{TDU}(M_C || M_S || Q_A, \widehat{M}_L || M_S || Q_A, \widehat{M}_L || M_S || Q_A, G)_{[T_c:T_c+T_s+T_a]} \quad (4)$$

where $||$ represents concatenation.

4.3. Memory-Refined Decoder

Previous works [21, 45] have highlighted the benefits of using anticipation in detection; however, they introduce learning biases when utilizing pseudo-future information. To address this, we design a near-future generator in the decoder that is independent of short-term memory. Our decoder also incorporates a memory refinement module that refines the encoded short-term memory from the Context-Enhanced encoder using the generated near-future context.

Near-Future Generator. In Sec. 3.3, we demonstrated that near-future information boosts intermediate frames’ performance through non-causal leakage. However, current method [45] provides near-future ($t+1 \sim t+\tau$) via anticipation only for the current frame t , not earlier ones. To address this, we propose the Near-Future Generator, which generates near-future information for all short-term frames. In addition, we avoid using short-term memory and instead leverage compressed long-term to generate near-future for all frames in short-term. The use of compressed long-term eliminates the non-causal leakage outlined in Sec. 3.3. Specifically, a TDU with learnable queries Q_F of length T_f retrieves useful information from compressed long-term \widehat{M}_L . The generated future M_F spans from t_s to $t_s + T_f$, providing near-future information for all short-term frames.

$$M_F = \text{TDU}(Q_F, \widehat{M}_L, \widehat{M}_L, \text{None}). \quad (5)$$

Memory Refinement. We refine the encoded short-term and anticipation M_{SA} from the Context-Enhanced encoder with the generated near-future M_F . The memory refinement module takes M_{SA} as queries and the fusion of long \widehat{M}_L , short M_{SA} and near-future M_F as keys and values for memory refinement. Since M_F is generated based upon the compressed long-term \widehat{M}_L , using it to update M_{SA} avoids contamination from indirectly accessing subsequent frames. The refined memory \widehat{M}_{SA} is then passed to a classifier for action detection and anticipation.

$$\widehat{M}_{SA} = \text{TDU}(M_{SA}, \widehat{M}_L || M_{SA} || M_F, \widehat{M}_L || M_{SA} || M_F, G). \quad (6)$$

4.4. Training and Inference

Following prior works [45, 51, 55], training samples are generated using a sliding window (THUMOS’14 and CrossTask) with a random start and stride T_s , or event-based sampling (EK100). The Context-Enhanced Encoder M_{SA} and Memory-Refined Decoder \widehat{M}_{SA} predictions are fed into a shared classifier, yielding action probabilities P_{SA} and \widehat{P}_{SA} . Cross-entropy loss is applied to the entire short-term memory and the anticipation based on ground truth labels Y_{SA} :

$$\mathcal{L}_{SA}^0 = - \sum_{i=1}^{T_s+T_a} Y_{SA}^i \log P_{SA}^i, \quad \mathcal{L}_{SA}^1 = - \sum_{i=1}^{T_s+T_a} Y_{SA}^i \log \widehat{P}_{SA}^i \quad (7)$$

Additionally, the generated future features, M_F , are passed through the same classifier, yielding the probability, P_F , based on the future targets, Y_F :

$$\mathcal{L}_F = - \sum_{i=1}^{T_f} Y_F^i \log P_F^i \quad (8)$$

The final training loss is defined as

$$\mathcal{L} = \mathcal{L}_{SA}^1 + \lambda_1 \mathcal{L}_{SA}^0 + \lambda_2 \mathcal{L}_F \quad (9)$$

where λ_1 and λ_2 are the balancing coefficients.

During inference, samples are generated with a sliding window (stride 1, start time 0) to simulate online streaming setup. Detection and anticipation are inferred simultaneously from \widehat{P}_{SA} of the Memory-Refinement module, with outputs split as $\widehat{P}_S = \widehat{P}_{SA[:T_s]}$, and $\widehat{P}_A = \widehat{P}_{SA[T_s:T_s+T_a]}$. For detection, only the last frame prediction in \widehat{P}_S is used for action detection. For anticipation, the corresponding frame in \widehat{P}_A is selected based on the time gap τ for forecasting.

5. Experiments

5.1. Dataset, Evaluation, and Implementation

Dataset. We experiment on three datasets: THUMOS’14(TH’14) [22], EPIC-Kitchens-100 (EK100) [9], and CrossTask(CT) [57]. Each dataset has unique characteristics. THUMOS’14 is sparsely annotated, with most videos containing a single action; EK100 contains fine-grained actions where long-term dependencies are less critical; CrossTask features procedural videos with strong temporal action relationships. THUMOS’14 includes 413 untrimmed sports videos annotated with 20 classes. Following [45, 50, 51], we train on the validation set (200 videos) and evaluate on the test set (213 videos). EK100 contains 100 hours of egocentric kitchen videos, labeled with 97 verb classes, 300 noun classes, and 3806 action classes. We adopt the train/val split from [16]. CrossTask contains 2750 videos of 18 primary tasks comprising 212 hours of video with 105 action classes. **Evaluation.** Though our work targets OAD, CMERT effectively handles detection and anticipation in a unified way, so

Table 1. Length of each partitioned context in seconds, including long-term, short-term, anticipation, near-past and near-future.

Dataset	Long	Short	Anticipation	Near-past	Near-future
TH'14	256	4	2	0.5	12
EK100	128	8	2	2	8
CrossTask	128	10	2	8	12

we report results for both detection and anticipation. Following [11, 45, 51, 55], we evaluate online action detection and anticipation using per-frame mean average precision (mAP) for THUMOS'14 and CrossTask, and mean Top-5 Recall for verb/noun/action in EK100. For anticipation, we apply a period ranging from 0.25s to 2.0s with a stride of 0.25s for THUMOS'14, and a fixed interval of 1s for EK100 [45].

Implementation. We use pre-extracted frame features as in [45, 51, 55]. For THUMOS'14, we employ two-stream features (at 4 FPS) with ResNet-50 for visuals and BN-Inception for motion [5, 51, 55]. On EK100, we use features from a two-stream TSN (4 FPS) pretrained on ImageNet [16, 55]. For CrossTask, we incorporate RGB I3D [5] features at 1 FPS with audio VGG features [57]. Tab. 1 provides the lengths of the partitioned long-term, short-term, anticipation, near-past, and near-future contexts. For the two-stage long-term compression, we set the number of queries to 16-32 for THUMOS'14 and CrossTask, and 16-16 for EK100. Balancing coefficients λ_1 and λ_2 in Eq. (9) are 0.2 and 0.5, respectively. Similar to [45, 55], we use the Adam optimizer with weight decay and a cosine annealing schedule with warm-up. For EK100, we adopt equalization loss [43] to address the long-tail action, along with MixClip [55] and MixClip++ [45] for data augmentation. Further details of hyperparameters are in Supplementary B.

Table 2. OAD performance comparison, measured by mAP for THUMOS'14 and CrossTask, and mean Top-5 Recall for EK100.

Method	TH'14	EK100				
		Method	CT	Verb	Noun	Action
LSTR [51]	69.5	LSTR [51]	33.0	39.6	44.1	22.6
GateHub [8]	70.7	Testra [55]	33.4	39.7	45.6	25.1
Testra [55]	71.2	MAT [45]	33.9	44.5	48.3	26.3
MAT [45]	71.6	MAT-rw	34.1	46.3	47.3	26.7
JOAAD [21]	72.6	MAT-stream	27.9	43.5	45.1	24.7
MAT-rw	71.7	CMeRT	35.9	47.1	48.3	27.6
MAT-stream	58.1					
CMeRT	73.2					

5.2. State-of-the-art Comparisons

5.2.1. Online Action Detection

We compare CMeRT with the state-of-the-art OAD methods on THUMOS'14, CrossTask and EK100 in Tab. 2. On THUMOS'14, our method outperforms memory-based methods LSTR [51], Testra [55], and MAT [45] by 3.7%, 2%, and 1.6% in mAP, respectively. It achieves state-of-the-art performance, surpassing the latest work [21] by 0.6% mAP. On CrossTask and EK100, our method also achieves state-of-

Table 3. Action anticipation results on THUMOS'14.

Method	mAP@ τ								Avg.
	0.25	0.50	0.75	1.0	1.25	1.50	1.75	2.0	
IJU [27]	55.6	55.3	54.6	53.1	51.4	49.8	48.5	46.9	51.9
LSTR [51]	60.4	58.6	56.0	53.3	50.9	48.9	47.1	45.7	52.6
Testra [55]	66.2	63.5	60.5	57.4	54.8	52.6	50.5	48.9	56.8
MAT [45]	-	-	-	-	-	-	-	-	58.2
CMeRT	69.9	66.6	63.2	60.1	57.3	54.9	52.8	50.9	59.5

Table 4. Action anticipation results on EK100, measured by class mean Top-5 Recall.

Method	Pre-train	Verb	Noun	Action
RULSTM [15]	IN-1K	27.8	30.8	14.0
TempAgg [37]	IN-1K	23.2	31.4	14.7
AVT [20]	IN-21K	28.2	32.0	15.9
Testra [55]	IN-1K	30.8	35.8	17.6
MAT [45]	IN-1K	35.0	38.8	19.5
CMeRT	IN-1K	35.1	39.7	19.8

Table 5. Ablation study of Context-Enhancement(CE) using near-past and Memory-Refinement(MR) using near-future in OAD.

CE	MR	TH'14	CrossTask	EK100		
				Verb	Noun	Action
\times	\times	71.5	33.4	44.9	26.9	26.3
\times	\checkmark	73.0	34.8	46.7	47.3	27.1
\checkmark	\times	71.9	33.9	46.0	47.6	26.6
\checkmark	\checkmark	73.2	35.9	47.1	48.3	27.6

the-art performance, improving mAP by 2% on CrossTask and Top-5 action recall by 1.3% on EK100.

We further test naive baselines to address the train-inference discrepancy, including a reweighting method, MAT-rw and a streaming training method, MAT-stream, based on the state-of-the-art model MAT [45]. For MAT-rw, a larger weight is assigned to the latest frame's loss. As learning in MAT is biased toward intermediate frames(Fig. 1(b)), reweighting the latest frame helps mitigate the bias, resulting in slight performance improvements. For MAT-stream, only the latest frame in the short-term is used for training, discarding other short-term frames to match inference. We adjust the batch size accordingly to ensure that MAT-stream receives the same number of updates each epoch as MAT. Results indicate a large performance drop, possibly due to increased batch diversity. Previously, a training batch contains frames from the same short-term memory with similar views and actions. Removing all but the latest frame increases diversity within the batch, complicating training. In addition, MAT-stream also increases the training cost, as an entire forward pass is needed for training on a single frame.

5.2.2. Action Anticipation

We compare our method to prior approaches on THUMOS'14 and EK100 for action anticipation in Tab. 3 and Tab. 4. Our method outperforms the state-of-the-art MAT [45] by 1.3% on THUMOS'14 and achieves competitive performance on EK100, particularly in noun and action

Table 6. Ablation study of near-past(N-past) length(sec.) for Context-Enhanced Encoder in OAD.

N-past	CrossTask	N-past	TH'14	EK100		
				Verb	Noun	Action
5	35.1	0.5	73.2	46.4	47.7	27.2
10	35.9	1	72.8	46.8	47.6	27.3
15	35.6	2	72.7	47.1	48.3	27.6
20	35.5	3	72.4	46.7	47.9	27.5

Table 7. Ablation study on near-future(N-fut) length(sec.) for Memory-Refinement module in OAD.

N-fut(s)	TH'14	CrossTask	EK100		
			Verb	Noun	Action
4	72.6	35.1	45.9	48.5	27.0
8	73.0	35.3	47.1	48.3	27.6
12	73.2	35.9	46.7	48.6	27.3
16	72.7	35.6	46.8	27.6	27.1

prediction, surpassing MAT by 0.9% and 0.3%, despite the dataset’s large scale and diverse categories. The results validate our method’s effectiveness in jointly modeling detection and anticipation. Anticipation can be further improved, but at the cost of detection due to the inherent task trade-off.

5.3. Ablation Studies

Contribution of Key Modules. We assess the contribution of the near-past context in the Context-Enhanced encoder and the near-future generation in the Memory-Refined decoder in Tab. 5. Incorporating near-future generation for refinement improves performance by 1.5%, 1.4%, and 0.8% on THUMOS’14, CrossTask, and EK100, respectively. Context enhancement further boosts performance by approximately 0.2% on THUMOS’14, 1.1% on CrossTask, and 0.5% on EK100. Combined, these two modules yield the best results.

Near-Past Context. The near-past context is introduced to enrich short-term memory with additional past context, especially for earlier frames. Results in Tab. 6 show the impact of near-past context length, indicating that a moderate length relative to short-term memory is optimal. The near-past length balances between enhancing early frame representations with more near-past context and providing data augmentation with less. A longer near-past length may lead to overfitting of the latest frame by giving it excessive context(both short-term and near-past context), while no near-past context results in hard training samples(these earlier frames), offering context-based data augmentation. For THUMOS’14, a shorter length of 0.5 seconds performs best, likely due to the dataset’s simplicity and overfitting risk. In contrast, CrossTask and EK100 benefit from a longer near-past length to capture complex action interactions.

Near-Future Context. The generated near-future enriches short-term memory with information beyond the past, enhancing detection. Tab. 7 shows the impact of near-future length, suggesting that an optimal length should exceed short-

term memory, enabling all short-term frames to access immediate future context. A length that’s too short fails to provide future information for the latest frames, while an overly long length makes long-horizon prediction challenging, potentially distracting detection learning and introducing noise.

Near vs. Distant Context. To highlight the importance of immediate context, we conduct ablation studies by replacing the near-past($t_s - T_c$ to t_s) and near-future(t_s to $t_s + T_f$) contexts with their distant counterparts. Specifically, we use distant-past from $t_s - T_c - T_s$ to $t_s - T_s$ and distant-future from t to $t + T_f$. The results in Tab. 8, demonstrate the importance of near-contexts over distant ones. Especially, distant future leads to a larger performance drop, as long-horizon anticipation is harder than the near one.

5.4. Runtime Analysis

We analyze computational complexity and runtime speed using a single NVIDIA RTX A4000 GPU on THUMOS’14. Focusing on runtime excluding preprocessing (i.e., without feature extraction), Tab. 9 compares model parameters, computational complexity, FPS, and performance. Compared to LSTR [51] and Testra [55], our model is larger and has higher computational cost due to near-future generation and memory refinement, resulting in lower FPS but yielding large performance gains. Against the SOTA MAT [45], which also uses generated future, our method is more efficient, achieving 24.6 FPS higher with a smaller model and reduced computational cost, while also delivering superior performance. Like [51], our method can further enhance online inference efficiency by storing intermediate results from the first compression stage, increasing FPS to 133.3.

5.5. Advancing OAD

State-of-the-art Features. Existing OAD works rely on outdated pre-extracted RGB features, e.g. ResNet or segment-wise features, e.g. I3D. Given advancements in vision foundation models [33, 53], we explore using the advanced DinoV2 [33] for feature extraction, evaluated on THUMOS’14 and CrossTask. As shown in Tab. 10, DinoV2 features yield performance gains of 3.2% and 11.4% on THUMOS’14 and CrossTask, respectively. Testing all memory-based methods with new features further confirms our method’s robustness, as it consistently outperforms others. Advanced features have promising implications for OAD research community, suggesting that models are not always the bottleneck; advancing the field requires consistently using state-of-the-art features that capture fine-grained details.

Table 8. Ablation study on near vs. distant contexts in OAD.

Past	Future	TH'14	CrossTask	EK100		
				Verb	Noun	Action
Near	Near	73.2	35.9	47.1	48.3	27.6
Near	Distant	72.9	35.0	46.6	47.8	27.0
Distant	Near	73.0	35.3	46.8	48.0	27.1

Table 9. Efficiency comparison on TH’14.

Method	#Param	GFLOPS	FPS	mAP
LSTR [51]	58.8	4.70	140.8	69.5
Testra [55]	58.9	4.72	135.1	71.2
MAT [45]	107.4	6.62	102.0	71.6
CMeRT	94.5	5.36	126.6	73.2

Table 10. Performance using DinoV2.

Method	TH’14		CrossTask	
	ResNet	Dino	I3D	Dino
LSTR [51]	69.5	74.3	33.0	45.1
Testra [55]	71.2	74.5	33.4	44.9
MAT [45]	71.6	75.3	33.9	46.8
CMeRT	73.2	76.4	35.9	47.3

Table 11. Online action detection with latency δ .

Latency	TH’14	CrossTask	EK100		
			Verb	Noun	Action
0s	73.2	35.9	47.1	48.3	27.6
0.25s	74.5	-	48.2	49.0	27.9
0.5s	75.4	-	48.9	49.5	28.2
1s	76.6	36.6	49.4	50.6	28.7
2s	76.7	36.9	49.7	50.4	29.3

Table 12. Benchmarking results with new protocols, including frame-wise(mAP and Rec@5) and event-wise(point-wise F1 score with threshold 1s(P-F1) and segment-wise F1 score with iou threshold 0.25(S-F1)) metrics, updated features, and latency models. For EK100, we report frame-wise performance for verb/noun/action(v/n/a), and event-wise performance only on actions.

Method	THUMOS’14				CrossTask				EK100				
	mAP	P-F1	Edit	S-F1	mAP	P-F1	Edit	S-F1	mAP(v/n/a)	Rec@5(v/n/a)	P-F1	Edit	S-F1
LSTR [51]	70.0	42.9	45.9	49.0	33.0	26.2	34.2	34.8	15.6/16.0/8.6	39.1/44.3/23.5	7.1	7.2	6.0
Testra [55]	71.2	42.7	44.4	47.3	33.4	25.0	34.0	33.7	16.4/18.3/9.8	41.1/45.8/25.1	8.1	8.0	7.2
MAT [45]	71.6	45.0	45.1	50.0	33.9	26.5	35.5	34.4	16.4/18.9/10.8	43.5/46.9/26.3	8.6	9.1	7.8
CMeRT	73.2	45.8	46.9	51.5	35.9	28.4	36.8	37.0	18.5/19.7/11.5	47.0/48.6/27.6	10.7	10.9	10.4
CMeRT Dinov2	76.4	47.8	49.1	52.8	47.3	35.4	44.5	44.9	-	-	-	-	-
CMeRT latency@1s	76.6	48.6	55.2	55.6	36.6	29.1	38.1	39.4	19.8/20.8/12.2	49.4/50.6/28.7	13.2	13.9	14.1

Sequence Metrics. While current methods are mainly evaluated frame-wise, understanding event-wise performance is equally crucial for OAD. High frame-wise accuracy can mask low event-wise accuracy, especially for short-duration actions and cases of oversegmentation [14, 36]. We encourage using event-based metrics inspired by start-point detection [18, 19] and temporal action segmentation [14, 35, 42, 52]: the Point-wise F1 score (1s threshold), Segment-wise F1 score (IoU threshold of 0.25), and the Edit score. Benchmarking memory-based methods in Tab. 12, CMeRT consistently outperforms others on both frame-wise and event-wise metrics, highlighting its superior robustness.

OAD with Latency. Observing the performance gains from indirect future access in intermediate short-term frames in Sec. 3.3, we explore the effect of directly accessing the future frames by introducing the future latency δ . Future latency δ enables predictions for frame $t - \delta$ at time t , providing a preview of the near future. It is valuable for applications that can tolerate delays or require post-prediction refinement. We introduce the first OAD baseline with future latency by replacing the causal mask with a new latency mask (see details in Suppl. C), enabling each short-term frame to access both past and near-future information up to a limit of δ . This immediate future context is essential, markedly boosting detection performance, as shown in Tab. 11. Even a slight latency, e.g. $\delta = 0.25s^3$ can lead to greater improvements.

5.6. Qualitative results

Fig. 5 shows the qualitative results for THUMOS’14. The bar charts compare the ground truth, predictions from MAT [45] and our method CMeRT. Our method addresses

learning biases, leading to more robust representations that better separate actions from the background or similar actions (*ThrowDiscus vs. Shotgun*). But, it struggles with short actions or small subjects in similar backgrounds (see more results in Supplementary D). These issues can be mitigated using advanced features that capture finer details.

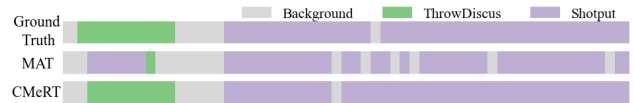


Figure 5. Quality results on THUMOS’14

6. Conclusion

This paper identifies the training-inference discrepancy in memory-based OAD methods, resulting in poor frame representations and learning biases in short-term memory. We propose the Context-Enhanced Memory-Refined Transformer (CMeRT) for joint detection and anticipation. CMeRT integrates near-past and near-future to provide additional immediate context, ensuring consistent learning across short-term frames. We also introduce a new OAD benchmark and protocols to better align with practical applications. Future efforts will explore trade-offs between detection and anticipation within the unified framework, and leveraging prior knowledge to capture high-level temporal dependencies.

Acknowledgment. This research is supported by the National Research Foundation, Singapore and DSO National Laboratories under its AI Singapore Programme (AISG Award No: AISG2-RP-2020-016). Any opinions, findings and conclusions or recommendations expressed in this material are those of the author(s) and do not reflect the views of National Research Foundation, Singapore.

³Features are extracted at 4 FPS, with average action durations of 4.9s(THUMOS’14) and 3.3s(EK100). A 0.25s delay equals to just 1 frames.

References

- [1] Dosovitskiy Alexey. An image is worth 16x16 words: Transformers for image recognition at scale. *arXiv preprint arXiv:2010.11929*, 2020. 2
- [2] Joungbin An, Hyolim Kang, Su Ho Han, Ming-Hsuan Yang, and Seon Joo Kim. Miniroad: Minimal rnn framework for online action detection. In *Proceedings of the IEEE/CVF International Conference on Computer Vision*, pages 10341–10350, 2023. 2
- [3] Anurag Arnab, Mostafa Dehghani, Georg Heigold, Chen Sun, Mario Lučić, and Cordelia Schmid. Vivit: A video vision transformer. In *Proceedings of the IEEE/CVF international conference on computer vision*, pages 6836–6846, 2021. 2
- [4] Yizhak Ben-Shabat, Xin Yu, Fatemeh Saleh, Dylan Campbell, Cristian Rodriguez-Opazo, Hongdong Li, and Stephen Gould. The ikea asm dataset: Understanding people assembling furniture through actions, objects and pose. In *Proceedings of the IEEE/CVF Winter Conference on Applications of Computer Vision*, pages 847–859, 2021. 1
- [5] Joao Carreira and Andrew Zisserman. Quo vadis, action recognition? a new model and the kinetics dataset. In *proceedings of the IEEE Conference on Computer Vision and Pattern Recognition*, pages 6299–6308, 2017. 6
- [6] Dibyadip Chatterjee, Fadime Sener, Shugao Ma, and Angela Yao. Opening the vocabulary of egocentric actions. *Advances in Neural Information Processing Systems*, 36:33174–33187, 2023. 2
- [7] Guo Chen, Yin-Dong Zheng, Jiahao Wang, Jilan Xu, Yifei Huang, Junting Pan, Yi Wang, Yali Wang, Yu Qiao, Tong Lu, et al. Videollm: Modeling video sequence with large language models. *arXiv preprint arXiv:2305.13292*, 2023. 2
- [8] Junwen Chen, Gaurav Mittal, Ye Yu, Yu Kong, and Mei Chen. Github: Gated history unit with background suppression for online action detection. In *Proceedings of the IEEE/CVF Conference on Computer Vision and Pattern Recognition*, pages 19925–19934, 2022. 1, 2, 6
- [9] Dima Damen, Hazel Doughty, Giovanni Maria Farinella, Antonino Furnari, Evangelos Kazakos, Jian Ma, Davide Moltisanti, Jonathan Munro, Toby Perrett, Will Price, et al. Rescaling egocentric vision: Collection, pipeline and challenges for epic-kitchens-100. *International Journal of Computer Vision*, pages 1–23, 2022. 5
- [10] Roeland De Geest and Tinne Tuytelaars. Modeling temporal structure with lstm for online action detection. In *2018 IEEE winter conference on applications of computer vision (WACV)*, pages 1549–1557. IEEE, 2018. 2
- [11] Roeland De Geest, Efstratios Gavves, Amir Ghodrati, Zhenyang Li, Cees Snoek, and Tinne Tuytelaars. Online action detection. In *Computer Vision—ECCV 2016: 14th European Conference, Amsterdam, The Netherlands, October 11–14, 2016, Proceedings, Part V 14*, pages 269–284. Springer, 2016. 6
- [12] Guodong Ding, Fadime Sener, Shugao Ma, and Angela Yao. Spatial and temporal beliefs for mistake detection in assembly tasks. *Computer Vision and Image Understanding*, page 104338, 2025. 1
- [13] Hyunjun Eun, Jinyoung Moon, Jongyoul Park, Chanho Jung, and Changick Kim. Learning to discriminate information for online action detection. In *Proceedings of the IEEE/CVF conference on computer vision and pattern recognition*, pages 809–818, 2020. 2
- [14] Yazan Abu Farha and Jurgen Gall. Ms-tcn: Multi-stage temporal convolutional network for action segmentation. In *Proceedings of the IEEE/CVF conference on computer vision and pattern recognition*, pages 3575–3584, 2019. 8
- [15] Antonino Furnari and Giovanni Maria Farinella. What would you expect? anticipating egocentric actions with rolling-unrolling lstms and modality attention. In *Proceedings of the IEEE/CVF International conference on computer vision*, pages 6252–6261, 2019. 6
- [16] Antonino Furnari and Giovanni Maria Farinella. Rolling-unrolling lstms for action anticipation from first-person video. *IEEE transactions on pattern analysis and machine intelligence*, 43(11):4021–4036, 2020. 5, 6
- [17] Jiyang Gao, Zhenheng Yang, and Ram Nevatia. Red: Reinforced encoder-decoder networks for action anticipation. *arXiv preprint arXiv:1707.04818*, 2017. 2
- [18] Mingfei Gao, Mingze Xu, Larry S Davis, Richard Socher, and Caiming Xiong. Startnet: Online detection of action start in untrimmed videos. In *Proceedings of the IEEE/CVF international conference on computer vision*, pages 5542–5551, 2019. 2, 8
- [19] Mingfei Gao, Yingbo Zhou, Ran Xu, Richard Socher, and Caiming Xiong. Woad: Weakly supervised online action detection in untrimmed videos. In *Proceedings of the IEEE/CVF conference on computer vision and pattern recognition*, pages 1915–1923, 2021. 8
- [20] Rohit Girdhar and Kristen Grauman. Anticipative video transformer. In *Proceedings of the IEEE/CVF international conference on computer vision*, pages 13505–13515, 2021. 6
- [21] Mohammed Guermal, Abid Ali, Rui Dai, and Francois Bremond. Joadaa: joint online action detection and action anticipation. In *Proceedings of the IEEE/CVF Winter Conference on Applications of Computer Vision*, pages 6889–6898, 2024. 1, 2, 3, 5, 6
- [22] Haroon Idrees, Amir R Zamir, Yu-Gang Jiang, Alex Gorban, Ivan Laptev, Rahul Sukthankar, and Mubarak Shah. The thumos challenge on action recognition for videos “in the wild”. *Computer Vision and Image Understanding*, 155:1–23, 2017. 5
- [23] Jinkyu Kim, Teruhisa Misu, Yi-Ting Chen, Ashish Tawari, and John Canny. Grounding human-to-vehicle advice for self-driving vehicles. In *Proceedings of the IEEE/CVF conference on computer vision and pattern recognition*, pages 10591–10599, 2019. 1
- [24] Young Hwi Kim, Seonghyeon Nam, and Seon Joo Kim. Temporally smooth online action detection using cycle-consistent future anticipation. *Pattern Recognition*, 116:107954, 2021. 2
- [25] Hema S Koppula and Ashutosh Saxena. Anticipating human activities using object affordances for reactive robotic response. *IEEE transactions on pattern analysis and machine intelligence*, 38(1):14–29, 2015. 1

- [26] Anna Kukleva, Fadime Sener, Edoardo Remelli, Bugra Tekin, Eric Sauser, Bernt Schiele, and Shugao Ma. X-mic: Cross-modal instance conditioning for egocentric action generalization. In *Proceedings of the IEEE/CVF Conference on Computer Vision and Pattern Recognition*, pages 26364–26373, 2024. 2
- [27] Sumin Lee, Hyunjun Eun, Jinyoung Moon, Seokeon Choi, Yoonhyung Kim, Chanho Jung, and Changick Kim. Learning to discriminate information for online action detection: Analysis and application. *IEEE Transactions on Pattern Analysis and Machine Intelligence*, 45(5):5918–5934, 2022. 6
- [28] Junnan Li, Dongxu Li, Silvio Savarese, and Steven Hoi. Blip-2: Bootstrapping language-image pre-training with frozen image encoders and large language models. In *International conference on machine learning*, pages 19730–19742. PMLR, 2023. 2
- [29] Yanghao Li, Cuiling Lan, Junliang Xing, Wenjun Zeng, Chunfeng Yuan, and Jiaying Liu. Online human action detection using joint classification-regression recurrent neural networks. In *Computer Vision–ECCV 2016: 14th European Conference, Amsterdam, The Netherlands, October 11–14, 2016, Proceedings, Part VII 14*, pages 203–220. Springer, 2016. 2
- [30] Bin Lin, Yang Ye, Bin Zhu, Jiaxi Cui, Munan Ning, Peng Jin, and Li Yuan. Video-llava: Learning united visual representation by alignment before projection. *arXiv preprint arXiv:2311.10122*, 2023. 2
- [31] Xiaolong Liu, Qimeng Wang, Yao Hu, Xu Tang, Shiwei Zhang, Song Bai, and Xiang Bai. End-to-end temporal action detection with transformer. *IEEE Transactions on Image Processing*, 31:5427–5441, 2022. 2
- [32] Ze Liu, Yutong Lin, Yue Cao, Han Hu, Yixuan Wei, Zheng Zhang, Stephen Lin, and Baining Guo. Swin transformer: Hierarchical vision transformer using shifted windows. In *Proceedings of the IEEE/CVF international conference on computer vision*, pages 10012–10022, 2021. 2
- [33] Maxime Oquab, Timothée Darcet, Théo Moutakanni, Huy Vo, Marc Szafraniec, Vasil Khalidov, Pierre Fernandez, Daniel Haziza, Francisco Massa, Alaaeldin El-Nouby, et al. Dinov2: Learning robust visual features without supervision. *arXiv preprint arXiv:2304.07193*, 2023. 2, 7, 1
- [34] Guansong Pang, Cheng Yan, Chunhua Shen, Anton van den Hengel, and Xiao Bai. Self-trained deep ordinal regression for end-to-end video anomaly detection. In *Proceedings of the IEEE/CVF conference on computer vision and pattern recognition*, pages 12173–12182, 2020. 1
- [35] Zhanzhong Pang, Fadime Sener, Shrinivas Ramasubramanian, and Angela Yao. Cost-sensitive learning for long-tailed temporal action segmentation. In *BMVC*, 2024. 2, 8
- [36] Zhanzhong Pang, Fadime Sener, Shrinivas Ramasubramanian, and Angela Yao. Long-tail temporal action segmentation with group-wise temporal logit adjustment. In *European Conference on Computer Vision*, pages 320–338. Springer, 2024. 2, 8
- [37] Fadime Sener, Dipika Singhania, and Angela Yao. Temporal aggregate representations for long-range video understanding. In *Computer Vision–ECCV 2020: 16th European Conference, Glasgow, UK, August 23–28, 2020, Proceedings, Part XVI 16*, pages 154–171. Springer, 2020. 6
- [38] Fadime Sener, Dibiyadip Chatterjee, Daniel Shelepov, Kun He, Dipika Singhania, Robert Wang, and Angela Yao. Assembly101: A large-scale multi-view video dataset for understanding procedural activities. In *Proceedings of the IEEE/CVF Conference on Computer Vision and Pattern Recognition*, pages 21096–21106, 2022. 1
- [39] Fadime Sener, Rishabh Saraf, and Angela Yao. Transferring knowledge from text to video: Zero-shot anticipation for procedural actions. *IEEE transactions on pattern analysis and machine intelligence*, 45(6):7836–7852, 2022. 1
- [40] Zheng Shou, Junting Pan, Jonathan Chan, Kazuyuki Miyazawa, Hassan Mansour, Anthony Vetro, Xavier Giro-i Nieto, and Shih-Fu Chang. Online detection of action start in untrimmed, streaming videos. In *Proceedings of the European conference on computer vision (ECCV)*, pages 534–551, 2018. 2
- [41] Tianmin Shu, Dan Xie, Brandon Rothrock, Sinisa Todorovic, and Song Chun Zhu. Joint inference of groups, events and human roles in aerial videos. In *Proceedings of the IEEE conference on computer vision and pattern recognition*, pages 4576–4584, 2015. 1
- [42] Dipika Singhania, Rahul Rahaman, and Angela Yao. C2f-tcn: A framework for semi-and fully-supervised temporal action segmentation. *IEEE Transactions on Pattern Analysis and Machine Intelligence*, 45(10):11484–11501, 2023. 8
- [43] Jingru Tan, Changbao Wang, Buyu Li, Quanquan Li, Wanli Ouyang, Changqing Yin, and Junjie Yan. Equalization loss for long-tailed object recognition. In *Proceedings of the IEEE/CVF conference on computer vision and pattern recognition*, pages 11662–11671, 2020. 6
- [44] A Vaswani. Attention is all you need. *Advances in Neural Information Processing Systems*, 2017. 1, 4, 5
- [45] Jiahao Wang, Guo Chen, Yifei Huang, Limin Wang, and Tong Lu. Memory-and-anticipation transformer for online action understanding. In *Proceedings of the IEEE/CVF International Conference on Computer Vision*, pages 13824–13835, 2023. 1, 2, 3, 4, 5, 6, 7, 8
- [46] Limin Wang, Yuanjun Xiong, Zhe Wang, Yu Qiao, Dahua Lin, Xiaoou Tang, and Luc Van Gool. Temporal segment networks: Towards good practices for deep action recognition. In *European conference on computer vision*, pages 20–36. Springer, 2016. 2
- [47] Shiguang Wang, Zhizhong Li, Yue Zhao, Yuanjun Xiong, Limin Wang, and Dahua Lin. Denseflow, 2020. <https://github.com/open-mmlab/denseflow>. 1
- [48] Wenhai Wang, Enze Xie, Xiang Li, Deng-Ping Fan, Kaitao Song, Ding Liang, Tong Lu, Ping Luo, and Ling Shao. Pyramid vision transformer: A versatile backbone for dense prediction without convolutions. In *Proceedings of the IEEE/CVF international conference on computer vision*, pages 568–578, 2021. 2
- [49] Xiang Wang, Shiwei Zhang, Zhiwu Qing, Yuanjie Shao, Zhengrong Zuo, Changxin Gao, and Nong Sang. Oadtr: Online action detection with transformers. In *Proceedings of the IEEE/CVF International Conference on Computer Vision*, pages 7565–7575, 2021. 2
- [50] Mingze Xu, Mingfei Gao, Yi-Ting Chen, Larry S Davis, and David J Crandall. Temporal recurrent networks for online ac-

- tion detection. In *Proceedings of the IEEE/CVF international conference on computer vision*, pages 5532–5541, 2019. 2, 5
- [51] Mingze Xu, Yuanjun Xiong, Hao Chen, Xinyu Li, Wei Xia, Zhuowen Tu, and Stefano Soatto. Long short-term transformer for online action detection. *Advances in Neural Information Processing Systems*, 34:1086–1099, 2021. 1, 2, 3, 4, 5, 6, 7, 8
- [52] Fangqiu Yi, Hongyu Wen, and Tingting Jiang. As-former: Transformer for action segmentation. *arXiv preprint arXiv:2110.08568*, 2021. 8
- [53] Xiaohua Zhai, Basil Mustafa, Alexander Kolesnikov, and Lucas Beyer. Sigmoid loss for language image pre-training. In *Proceedings of the IEEE/CVF International Conference on Computer Vision*, pages 11975–11986, 2023. 7
- [54] Chen-Lin Zhang, Jianxin Wu, and Yin Li. Actionformer: Localizing moments of actions with transformers. In *European Conference on Computer Vision*, pages 492–510. Springer, 2022. 2
- [55] Yue Zhao and Philipp Krähenbühl. Real-time online video detection with temporal smoothing transformers. In *European Conference on Computer Vision*, pages 485–502. Springer, 2022. 1, 2, 3, 4, 5, 6, 7, 8
- [56] Luowei Zhou, Chenliang Xu, and Jason Corso. Towards automatic learning of procedures from web instructional videos. In *Proceedings of the AAAI Conference on Artificial Intelligence*, 2018. 1
- [57] Dimitri Zhukov, Jean-Baptiste Alayrac, Ramazan Gokberk Cinbis, David Fouhey, Ivan Laptev, and Josef Sivic. Cross-task weakly supervised learning from instructional videos. In *Proceedings of the IEEE/CVF Conference on Computer Vision and Pattern Recognition*, pages 3537–3545, 2019. 5, 6

Context-Enhanced Memory-Refined Transformer for Online Action Detection

Supplementary Material

A. Diagnising Context Modeling for OAD

Existing methods [45, 51, 55] suffer from a training-inference discrepancy, causing short-term context imbalance and a non-causal leakage during anticipation, resulting in learning biases. Fig. 6 shows the learning biases present in existing works from a performance perspective.

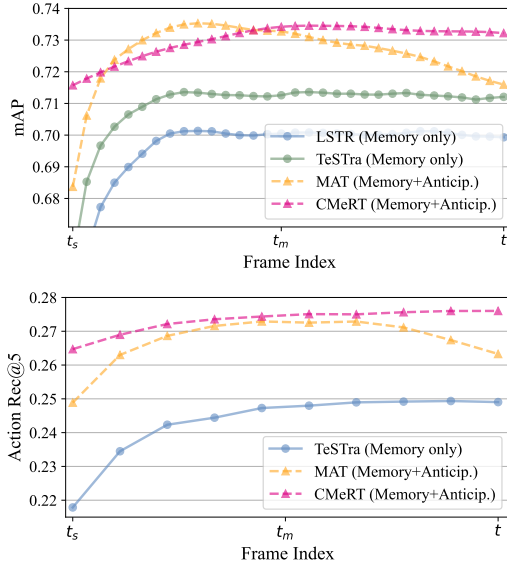


Figure 6. Frame performance within the short-term memory on THUMOS’14(top) and EK100(bottom).

First, we observe that early frames in the short-term memory are poorly learned, resulting in significantly lower performance. These poorly represented frames serve as low-quality samples, impairing the learning of classifier to effectively predict the latest frame. In contrast, CMeRT improves performance for early frames, though a performance gap still remains compared to the latest frame. The remaining gap is due to the use of a shorter near-past context, which limits the amount of context available to earlier frames compared to the latest one. Our empirical findings demonstrate that shorter near-past contexts are more beneficial, as they act as a form of data augmentation by exposing frames to less context. Naive approaches [45, 51, 55] that omit near-past context can also be seen as a form of data augmentation. However, they over-augment the data, introducing poor training samples that hamper the learning process.

Second, the performance curve of the anticipation-based method MAT [45] confirms the presence of non-causal leakage, as it shows significantly higher performance for intermediate frames compared to the latest frame. CMeRT however, effectively mitigate this leakage and learning bias, prioritizing the learning of the latest frame.

B. Experiments

Hyperparameters. The hyperparameters used for each dataset are summarized in Tab. 13.

Table 13. Hyperparameters for different experimental settings.

	THUMOS’14	CrossTask	EK100
batch size	32	32	32
epoch	12	12	12
warmup	8	5	10
learning rate	2e-4	7e-5	7e-5
weight decay	5e-5	1e-5	1e-4

MAT-rw and MAT-stream. We implement MAT-rw and MAT-stream based on the state-of-the-art memory-based model MAT [45] to evaluate standard approaches for addressing the training-inference discrepancy.

In MAT-rw, we assign a higher weight to the loss of the latest frame to mitigate the learning bias towards intermediate frames. Specifically, the weight is set to 1.2 for THUMOS’14 and 3.0 for CrossTask and EK100.

In MAT-stream, only the latest frame in the short-term memory is used for training, while other short-term frames are discarded to align with the inference. we modify the sliding window sampling by setting the stride to 1, ensuring all video frames are used for training. However, this increases the training set size compared to using a stride equal to the short-term memory length, resulting in more training samples and updates per epoch than the standard MAT. To mitigate this, we adjust the batch size to match the number of updates per epoch as in MAT [45].

C. Advancing OAD

DinoV2 Features. We use the Dinov2 ViT-g/14 model [33] to extract advanced RGB features for THUMOS’14 and CrossTask. We replace only the RGB features while other features, such as optical flow, remain unchanged. For THUMOS’14, following [51], we extract video frames at a rate of 24 FPS and divide the video into chunks of 6 frames, using the intermediate frame of each chunk for RGB feature extraction. The feature extraction is performed at the chunk level, meaning evaluation occurs every 0.25 seconds. The feature encoding process for CrossTask is similar to THUMOS’14, except that the chunk size is increased to 24 frames to align with the existing feature set.

While the advanced feature extractor improves performance, it also increases the computational burden. Following [51], we report the runtime for end-to-end online inference on THUMOS’14, including two-stream feature extraction in Tab. 14. Specifically, DenseFlow [47] is used to compute

optical flow, while RGB features are extracted using either ResNet52 [46] or the DinoV2 model. The results in Tab. 14 align with prior works [45, 51], confirming that optical flow remains the primary speed bottleneck. Compared to optical flow feature, the runtime for DinoV2 RGB feature extraction remains manageable. However, the DinoV2 model inference can be further accelerated through techniques such as model distillation, model weights quantization or conversion to Optimized formats, like TorchScript and ONNX. Model inference optimization is already a well-established practice in the industry, providing significant opportunities to leverage more advanced features while maintaining efficiency.

Table 14. Efficiency analysis of feature extraction on THUMOS’14. The performance is reported in frames per second(FPS)

Optical Flow		RGB	
Computation	Extraction	ResNet52	DinoV2
8.6	47.6	69.0	13.9

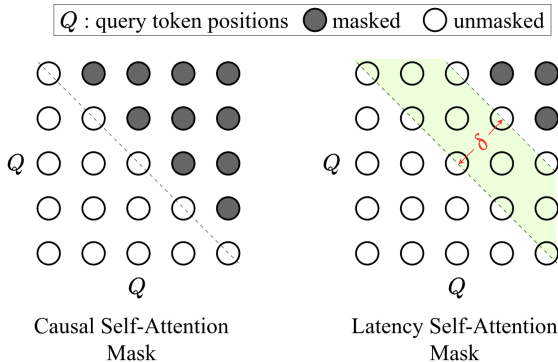


Figure 7. Self-attention masking to control query interactions.

OAD with latency For applications where delays are acceptable or post-prediction refinement is required, it is valuable to explore the advantages of incorporating limited future information into online action detection. To explore this, we introduce a future latency parameter, δ , and propose the first OAD baseline with future latency. Specifically, we construct base models based on TeTra [55], MAT [45], and our model CMeRT by replacing the causal mask in short-term self-attention with a new latency mask, as shown in Fig. 7. This new mask allows each short-term frame to additionally access the near-future information up to a limit of δ .

We evaluate the new OAD with latency setting using various base models and latency settings, with results in Fig. 8. Incorporating future latency improves performance across all models. Even a small latency, *e.g.* $\delta = 0.5$ can lead to greater improvements, with further gains expected as the latency increases. CMeRT consistently outperforms others by a large margin, demonstrating its robustness.

D. Qualitative Results

Fig. 9 and Fig. 10 show some qualitative results for THUMOS’14 and CrossTask, respectively. The bar charts present

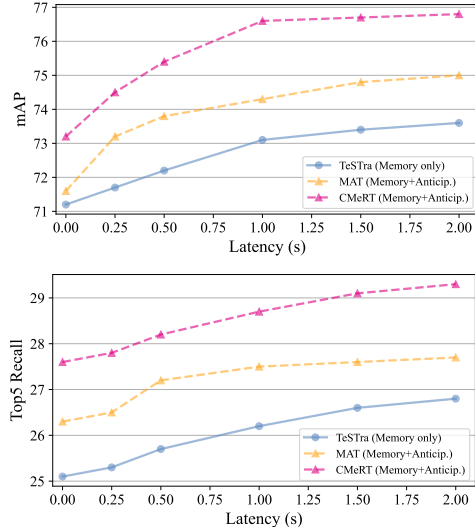


Figure 8. OAD performance under varied future latency on THUMOS’14(top) and EK100(bottom).

a comparison between the ground truth and the predictions from MAT [45] and our method CMeRT. The curve plots display the confidence in identifying the current true action. The results highlight that CMeRT effectively reduce the misclassification between background and foreground actions. Additionally, it improves the distinction between similar actions (*PoleVault vs. HighJump*). However, it struggles with short actions (*Whisk mixture & add coffee*) or small subjects in similar backgrounds (*SoccerPenalty*).

E. Extra Ablation Studies

Query configuration in the long-term compressor: We test on four query configurations (stage1-stage2): 16-16, 16-32, 32-32, and 32-64 on THUMOS’14. The mAP is 72.8%, 73.2%, 72.9%, and 72.8%, respectively. The results suggest that intermediate configurations are optimal, as excessive queries introduce noise and redundancy, while too few causes the loss of valuable information.

Short over long future: We designed the long-term memory (t_l to t_s) to generate a near-future (t_s to $t_s + T_f$) that overlaps and extends beyond the short memory to serve a pseudo-future for all short-term frames. Experimentally, generating a short near-future is favored over a longer one, as longer pseudo-futures are more challenging and costly, leading to degraded quality (Fig. 11). Even using the true future, performance saturates beyond a certain length (Fig. 12), which justifies our use of short-future generation.

Long-short division: We evaluate the impact of long-short term division on performance. As shown in Fig. 13, excessive long-term memory introduces noise, while insufficient long-term causes information loss. The short-term length has minimal impact if sufficient long-term is provided. Besides, near-future generation is less impacted by the division, since it always predicts the future following the long-term.

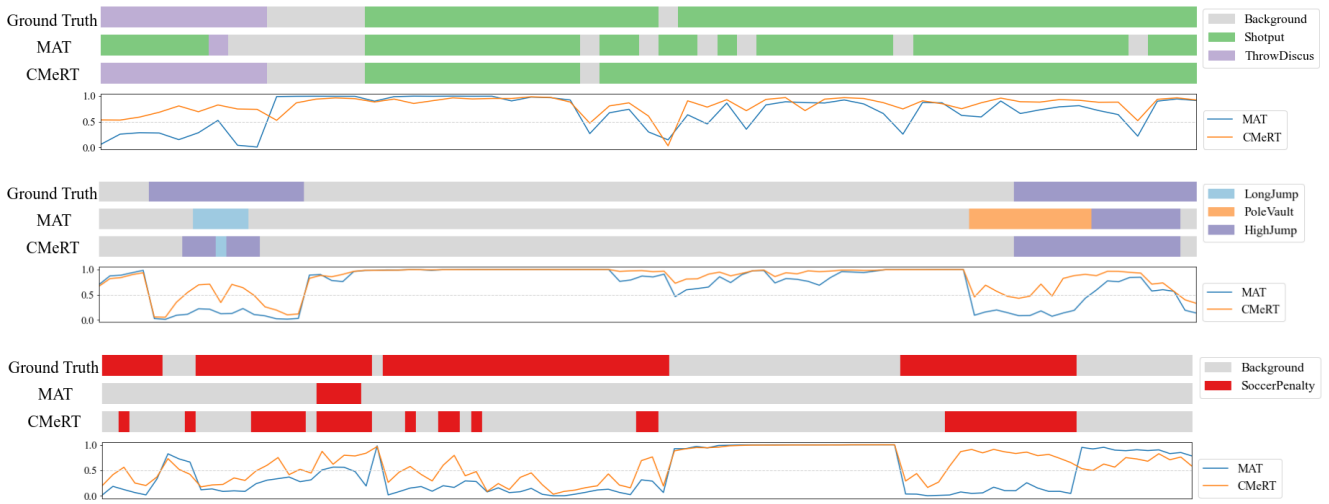


Figure 9. Quality results on THUMOS'14 - bar charts show predictions; curve plots for confidence of the true action.

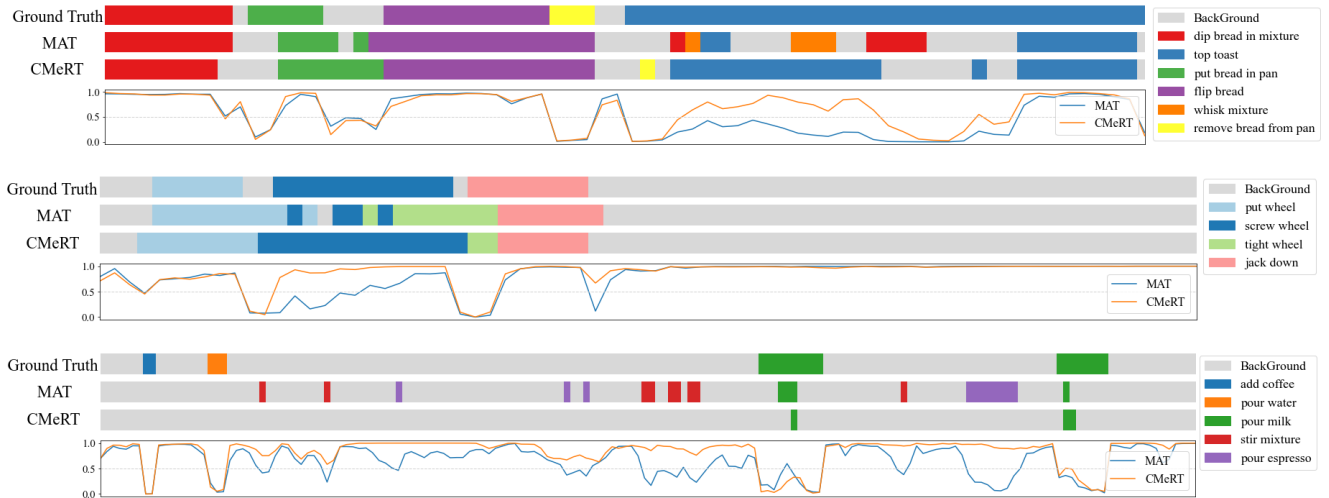


Figure 10. Quality results on CrossTask: top - Make French Toast, middle - Change a Tire, bottom - Make a Latte

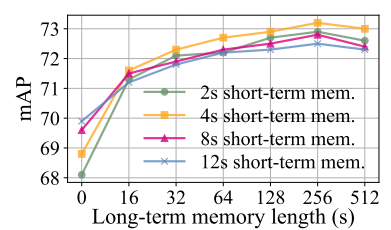
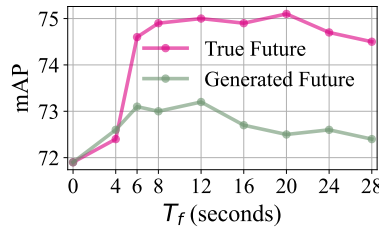
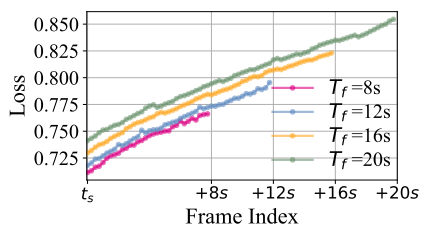


Figure 11. Extended future generation reduces quality (on THUMOS'14).

Figure 12. Distant future not helpful (on THUMOS'14).

Figure 13. Impact of long-short division on THUMOS'14.